Original Research Article

Journal of Tissue Engineering
Volume 15: 1–17
© The Author(s) 2024
Article reuse guidelines:
sagepub.com/journals-permissions
DOI: 10.1177/20417314241260436
journals.sagepub.com/home/tej
Sage

Delivery of dental pulp stem cells by an injectable ROS-responsive hydrogel promotes temporomandibular joint cartilage repair via enhancing anti-apoptosis and regulating microenvironment

Jinjin Ma[1#], Juan Li[1#], Shibo Wei[2], Qinwen Ge[4], Jie Wu[5], Leilei Xue[1], Yezi Qi[1], Siyi Xu[1], Hongting Jin[4], Changyou Gao[2,3] and Jun Lin[1]

Abstract

Temporomandibular joint (TMJ) cartilage repair poses a considerable clinical challenge, and tissue engineering has emerged as a promising solution. In this study, we developed an injectable reactive oxygen species (ROS)-responsive multifunctional hydrogel (RDGel) to encapsulate dental pulp stem cells (DPSCs/RDGel in short) for the targeted repair of condylar cartilage defect. The DPSCs/RDGel composite exhibited a synergistic effect in the elimination of TMJ OA (osteoarthritis) inflammation via the interaction between the hydrogel component and the DPSCs. We first demonstrated the applicability and biocompatibility of RDGel. RDGel encapsulation could enhance the anti-apoptotic ability of DPSCs by inhibiting P38/P53 mitochondrial apoptotic signal in vitro. We also proved that the utilization of DPSCs/RDGel composite effectively enhanced the expression of TMJOA cartilage matrix and promoted subchondral bone structure in vivo. Subsequently, we observed the synergistic improvement of DPSCs/RDGel composite on the oxidative stress microenvironment of TMJOA and its regulation and promotion of M2 polarization, thereby confirmed that M2 macrophages further promoted the condylar cartilage repair of DPSCs. This is the first time application of DPSCs/RDGel composite for the targeted repair of TMJOA condylar cartilage defects, presenting a novel and promising avenue for cell-based therapy.

Keywords

Hydrogel, temporomandibular arthritis, inflammation modulation

Date received: 10 April 2024; accepted: 23 May 2024

[1]Department of Stomatology, the First Affiliated Hospital, Zhejiang University School of Medicine, Hangzhou, China
[2]Innovation Center for Smart Medical Technologies & Devices, Binjiang Institute of Zhejiang University, Hangzhou, China
[3]MOE Key Laboratory of Macromolecular Synthesis and Functionalization Department of Polymer Science and Engineering, Zhejiang University, Hangzhou, China
[4]Institute of Orthopaedics and Traumatology of Zhejiang Province, The First Affiliated Hospital of Zhejiang Chinese Medical University (Zhejiang Provincial Hospital of Chinese Medicine), Hangzhou, Zhejiang, China
[5]School of Stomatology, Zhejiang Chinese Medical University, Hangzhou, China

[#]Authors contributed equally to this work

Corresponding authors:
Hongting Jin, Institute of Orthopaedics and Traumatology of Zhejiang Province, The First Affiliated Hospital of Zhejiang Chinese Medical University (Zhejiang Provincial Hospital of Chinese Medicine), No.54, Youdian Road, Shangcheng, Hangzhou, 310003, China.
Email: hongtingjin@163.com

Changyou Gao, Innovation Center for Smart Medical Technologies & Devices, Binjiang Institute of Zhejiang University, 66 Dongxin Avenue, Binjiang, Hangzhou, 310053, China.
Email: cygao@zju.edu.cn

Jun Lin, Department of Stomatology, the First Affiliated Hospital, Zhejiang University School of Medicine, 79 Qingchun Road, Shangcheng, Hangzhou, 310003, China.
Email: linjun2@zju.edu.cn

Creative Commons Non Commercial CC BY-NC: This article is distributed under the terms of the Creative Commons Attribution-NonCommercial 4.0 License (https://creativecommons.org/licenses/by-nc/4.0/) which permits non-commercial use, reproduction and distribution of the work without further permission provided the original work is attributed as specified on the SAGE and Open Access pages (https://us.sagepub.com/en-us/nam/open-access-at-sage).

Introduction

The temporomandibular joint (TMJ) is a multifaceted and heavily burdened articulation implicated in numerous craniofacial diseases and disorders.[1] Temporomandibular joint disorders (TMD) have emerged as one of the most prevalent musculoskeletal afflictions, affecting 5%–12% of the global population. Among the various subtypes of TMD, osteoarthritis (OA) is the most frequent and debilitating manifestation, characterized by the progressive degradation of the condylar cartilage within the TMJ. Despite of numerous therapeutic strategies for TMJ cartilage repair, an effective treatment is yet to be developed.[2] The current limitations in conventional TMJOA treatment have sparked interest in the burgeoning field of tissue-engineered cartilage regeneration.[3] Nevertheless, the development of suitable biomaterials for cartilage regeneration in TMJOA remains at an experimental stage.[3,4]

Cartilage has a unique tissue microenvironment, where efficacious biomaterial-mediated cartilage regeneration hinges on the complex biomaterial-host interactions, including modulation of immune responses and mesenchymal stem cells (MSC) differentiation. Macrophages serve as the primary immune cells to respond to invading pathogens, and their precise regulation of inflammation and tissue regeneration relying on the temporal and spatial distribution of M1 and M2 macrophage subgroups.[5] These subsets are identifiable by their characteristic marker molecules: IL-1β, CD86, and TNF-α for M1 macrophages, and Arg-1 and CD206 for M2 macrophages. At present, MSCs have garnered attention as "seed cells" in tissue engineering.[6,7] Stem cell-based therapies hold promise for treating TMJOA and regenerating full-thickness cartilage defects in the TMJ.[8,9]

Among various types of stem cells, dental pulp stem cells (DPSCs) demonstrate superior multipotency, proliferation rate, and accessibility compared to other counterparts such as bone marrow mesenchymal stem cells (BMSCs).[10] In particular, they can differentiate into chondrocytes, effectively maintaining the function and stability of cartilage.[11–13] DPSCs, TMJ discs, and mandibles all derive from neural crest.[14] Additionally, it is widely acknowledged that the composition of articular cartilage varies between the knee and TMJ joints, with a predominance of hyaline cartilage in the knee and fibrocartilage in the TMJ.[15] The report of Longoni et al. confirmed that DPSCs formed more fibrochondroid tissue than hyalinoid cartilage under various chondro-inductive conditions, which is more promising for the engineering of fibrochondroid tissue, such as TMJ.[16,17] So Given their ease of isolation, commendable expansion potential, and chondrogenic differentiation capability, DPSCs present a valuable prospect in articular cartilage tissue engineering.[18,19]

Despite the remarkable success achieved by MSC therapy in the treatment of TMJOA,[20] the challenge persists in attaining adequate therapeutic dosages precisely at the targeted site.[21] The survival capacity of transplanted MSCs within an inflammatory microenvironment is compromised, partially due to the oxidative stress following OA[22,23] that is intricately linked to the unstable TMJOA microenvironment.[24] Notably, ROS have been identified as potential OA pathogenic factors,[25,26] leading to cytotoxicity, inflammatory response and modulation of DPSCs differentiation.[27] Reactive oxygen species (ROS) acts as a REDOX-dependent inflammatory mediator, triggering macrophages to secrete TNF-α. Previous research also reported that mitochondrial functions and dynamics play a crucial role in determining the developmental trajectory of DPSCs. Prolonged exposure of DPSCs to H_2O_2 resulted in an elevation of ROS production, thereby compromising cell viability. Furthermore, ROS accumulation induces premature senescence in DPSCs.[5] Moreover, the differentiation of MSCs post-intra-articular injection is not adequately controlled, where the inflammation and oxidative stress significantly impede the differentiation process.[28] To address these challenges, a delivery system is needed to maintain the viability and function of transplanted stem cells. In this context, the cell-loaded hydrogels have been extensively employed in tissue engineering and regenerative medicine, mimicking the physical and chemical attributes of the extracellular microenvironment.[29–31]

The primary objective of this study is to enhance the efficacy of DPSCs for cartilage repair in TMJOA by utilizing our designed injectable ROS-responsive hydrogel (RDGel) as a stem cell delivery system. The RDGel acts as a physical barrier blocking the penetration of pro-inflammatory cells/cytokines, safeguarding DPSCs from immune system invasion, and enhancing their viability (Scheme 1). We shall assess the ability of DPSCs/RDGel composite to modify the inflammatory and immune microenvironment and to promote cartilage repair. The underlying mechanisms are also elucidated.

Materials and methods

Relevant details can be found in the supplementary document.

Results

Characterization of RDGel

The rheological and antioxidant properties, and cytotoxicity of RDGels at three different concentrations were measured and compared. Since the antioxidant properties of RDGels are HBPAK concentration-dependent, three different concentrations of HBPAK (10%, 15%, and 20%) were used for RDGel preparation. Rheological assessment of the RDGel at these concentrations at 37°C consistently demonstrated the higher storage moduli (G′) than the corresponding loss moduli (G″) throughout the investigated time scale, confirming the highly crosslinking nature of all

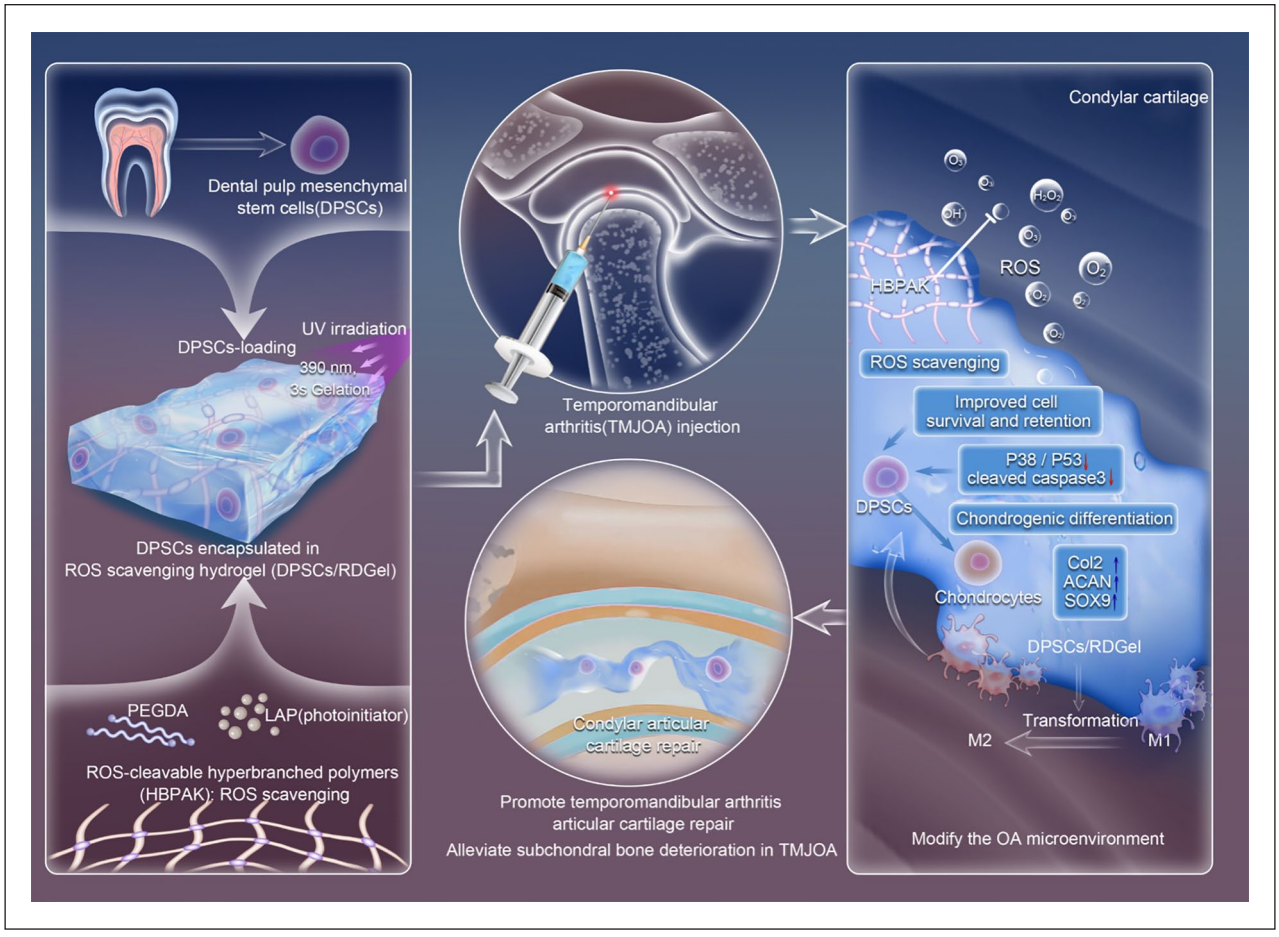

Scheme 1. Fabrication of the DPSC/RDGel composite for treating temporomandibular arthritis cartilage defects *in vivo*. The novel injectable hydrogel (RDGel) possessing reactive oxygen species (ROS) scavenging functionality exhibits the potential to augment anti-apoptotic capacity of dental pulp stem cells (DPSCs) under oxidative stress by suppressing the P38/P53 apoptotic signaling pathway, The synergistic effect of DPSCs/RDGel composites can improve the oxidative stress microenvironment, facilitate the polarization transformation of macrophages from M1 to M2, and subsequently augment the cartilage repair potential of DPSCs.

the RDGels. The storage modulus (G′) of 10% RDGel was significantly lower than those of the 15% and 20% counterparts, indicating more favorable injectability (Figure 1(a–c)). The antioxidant properties of the RDGel were evaluated through H_2O_2 and DPPH clearance. DPPH assay, an established method for assessing antioxidant potential in biomaterials, revealed that the radical scavenging was improved along with time prolongation for all the RDGel of different concentrations. However, the 20% RDGel had significantly higher scavenging ratio at the same time point (Figure 1(d and e)). In the H_2O_2 clearance experiment, there was no significant difference among the RDGel of different concentrations, where all the H_2O_2 were scavenged (Figure 1(f)). In summary, the HBPAK in the RDGel network plays a vital role in the ROS clearance. To mimic the characteristics of excessive ROS in the TMJOA microenvironment, two simulated environments, namely PBS and 250 mM H_2O_2/PBS, were established to evaluate the degradation performance of the prepared three RDGel. The mass of RDGel at various concentrations in 250 mM H_2O_2/PBS solution was lost over time with a much faster rate as compared to that in PBS solution. The 10% RDGel lost nearly 65% and 30% of their weight in 250 mM H_2O_2/PBS and PBS, respectively on day 12. The 15% RDGel and 20% RDGel exhibited a significant mass loss of approximately 60% in 250 mM H_2O_2/PBS by day 12. The slight degradation in PBS is attributed to the hydrolysis of β-amino ester bonds (Figure 1(g)). Next, a viability assay was conducted on DPSCs to assess the potential cytotoxicity of the RDGel. DPSCs demonstrated multipotent differentiation capacity into osteogenic, chondrogenic, and adipogenic lineages (Figure S1). The cytotoxicity of RDGels at different concentrations was assessed by culturing DPSCs (Figure S2 A-D) with RDGel extracts on day 1, day 3, day 5, and day 7, followed by CCK-8 assay. The cell viability of the 10% and 15% groups exhibited nearly 100% compared to the blank, indicating no cytotoxicity. In contrast, the cell viability was inhibited

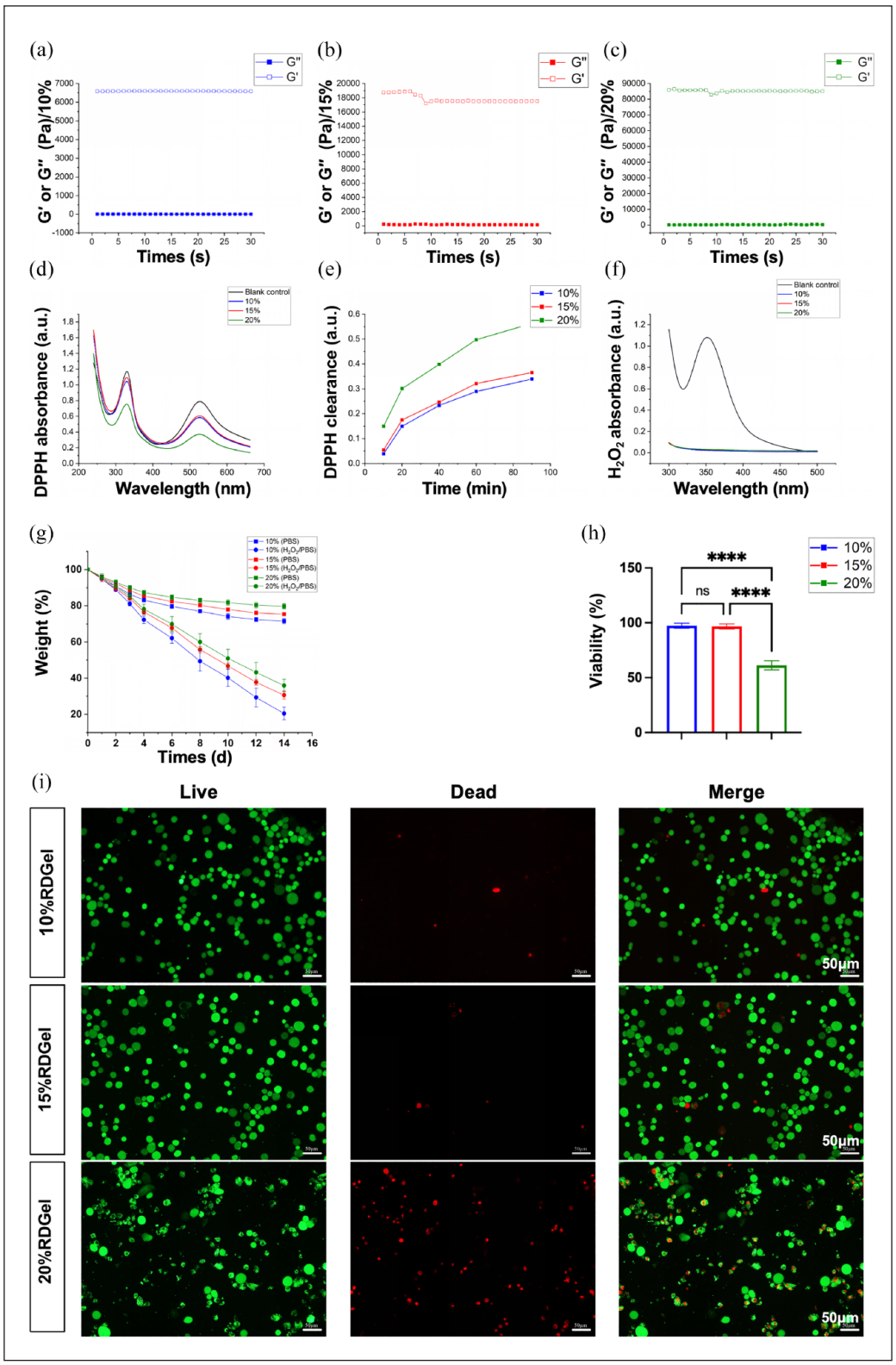

Figure 1. Characterization of RDGels at different concentrations. (a–c) Rheological properties of the RDGel with 10%, 15%, and 20% HBPAK concentrations. Time-sweep mode, temperature = 37°C, strain = 1%, frequency = 50 Hz. G′: storage modulus, and G″: loss modulus. (d) UV-vis spectroscopy of the RDGel with three different concentrations and blank control (absence of RDGel) in 200 μM DPPH ethanol solution. (e) DPPH clearance of the RDGel with three different concentrations overtime. (f) UV–vis spectroscopy of the RDGel with three different concentrations and blank control (absence of RDGel) in 500 μM H_2O_2/1 M KI solution. (g) Degradation of different concentrations of RDGels in PBS and 250 mM H_2O_2/PBS. (h and i) Representative live/dead staining images of DPSCs encapsulated with RDGel at three different concentrations on day 7, and statistical analysis. Mean ± SD is shown. $n = 3$. p-values are calculated using the one-way ANOVA with Tukey's post-test correction, ****$p < 0.0001$; ns, no significant difference.

significantly by the 20% RDGel. Additionally, the DPSCs were encapsulated in RDGels with concentrations of 10%, 15%, and 20% and cultured for 1–7 days. Subsequently, live/dead staining was performed to evaluate cell viability. The percentage of live cells in the 10% and 15% groups exceeded 80%, with no significant differences observed on day 1, day 3, day 5, and day 7. However, in the 20% group, there was a notable increase in the proportion of dead cells which escalated over time (Figure 1(h and i) and Figure S2 E). Considering all the results, the 10% RDGel was selected for further investigation.

The protective effect of 10% RDGel on DPSCs was assessed. Figure 2(b) shows that 10% RDGel possessed desirable injectable property, allowing administration through a syringe with a diameter of 0.30 mm. The porous structure of lyophilized 10% RDGel was apparent (Figure 2(c)) due to the lyophilization of the crystallized ice. In our system, the DPSCs are individually dispersed within the pores of the RDGel scaffolds (Figure 2(d)). For a more comprehensive assessment of the protective effects of RDGel under oxidative stress conditions, DPSCs were stained with a fluorescent probe, 2′,7′-dichlorofluorescin diacetate (DCFH-DA), to measure intracellular levels of ROS. After 1, 3, 5, and 7 days of H_2O_2 stimulation of DPSCs, the DCFH-DA working solution was added for staining. Subsequently, fluorescence microscopy was performed. In contrast to the H_2O_2 group, the group exposed to H_2O_2 exhibited a more pronounced green fluorescence due to the introduction of H_2O_2 caused oxidative damage, while the H_2O_2/RDGel group displayed a subdued green fluorescence, indicating that RDGel effectively inhibited oxidative stress of DPSCs (Figure 2(e and f), Figure S3). These findings indicate that the RDGel responsive to ROS could safeguard the DPSCs from oxidative stress in *vitro*.

RDGel encapsulation protects DPSCs from oxidative stress injury by inhibiting P38/P53 apoptosis pathway in vitro

To elucidate the underlying mechanism of RDGel action on DPSCs under oxidative stress, comprehensive mRNA sequencing was performed on DPSCs encapsulated with and without RDGel under 200 μM H_2O_2-induced oxidative stress. A volcano plot visually represents the significant differences in gene expression between the H_2O_2 and H_2O_2 + RDGel treatment groups. The analysis identified 1761 up-regulated and 687 down-regulated genes (Figure 3(a)). The KEGG enrichment analysis revealed that the differentially expressed genes were predominantly enriched in the MAPK signaling pathway, signaling pathways regulating pluripotency of stem cells, as well as P53 (Figure 3(b)). GO enrichment analysis of the above differentially expressed genes showed that in terms of cellular component, these differentially expressed genes were mainly located in the nucleus, cytoplasm, membrane, cytosol, and mitochondria (Figure 3(c)). In terms of biological process, it is mainly involved in apoptosis, cell differentiation, and protein phosphorylation (Figure 3(d)).

Subsequently, the potential mechanism was investigated. Our findings demonstrated that H_2O_2 stimulation induced a significant upregulation of p-p38/p38 and p-p53/p53 expression in DPSCs. Notably, the DPSCs/RDGel group exhibited a remarkable attenuation in the expression levels of these proteins following equivalent exposure to H_2O_2 when compared to the H_2O_2 group (Figure 3(e, g, and h)). Then, an array of apoptosis-related genes was analyzed, including Bcl2, Bax, and Cleaved caspase3. The H_2O_2 group exhibited a significant upregulation in cleaved caspase3 and Bax expression, along with a significant downregulation in Bcl2 expression, compared to the control group. However, compared to the H_2O_2 group, the RDGel encapsulating could significantly decrease the expression of cleaved caspase3 and Bax and increase the expression of Bcl2 in DPSCs after H_2O_2 treatment, with statistically significant differences (Figure 3(f, i–k)). Furthermore, the P38 receptor agonist anisomycin (ANI), known for effectively activating the P38 MAPK signaling pathway, verified the pathway is the target effector, as the addition of ANI reversed the protective effect of RDGel encapsulation. The expressions of pp-38, pp-53, Bcl2/Bax, and Cleaved caspase3 were significantly upregulated in the H_2O_2/RDGel + ANI group compared to the H_2O_2/RDGel group, exhibiting statistically significant differences (Figure 3(e–k)).

RDGel encapsulation improves the survival of transplanted DPSCs and promotes temporomandibular arthritis articular cartilage and subchondral bone repair in vivo

The RDGel can be rapidly formed within a brief duration of time (3 s) through mild UV irradiation in *vitro*. Moreover, it can be conveniently administered via an insulin needle for facile in vivo surgical procedures. The gelling mechanism of RDGel involves the photoinduced generation of LAP, which in turn generates free radicals. These free radicals then initiate the polymerization of HBPAK and PEGDA double bonds within the system, leading to the formation of cross-linked networks. The luciferase activity of the transplanted DPSCs was determined by the bioluminescence signal. The mean fluorescence intensity (MFI) of the DPSCs group displayed a gradual decrease from day 1 to day 14. In contrast, the MFI in the DPSCs/RDGel group increased on day 3, followed by a decline. Compared to that of the DPSCs group, the bioluminescence signal in the DPSCs/RDGel group was higher on day 1, day 3, day 5, day 7, and day 14, indicating enhanced cell survival post-transplantation (Figure 4(a and b)).

For the therapeutic intervention, intra-articular injections of different groups were administered weekly

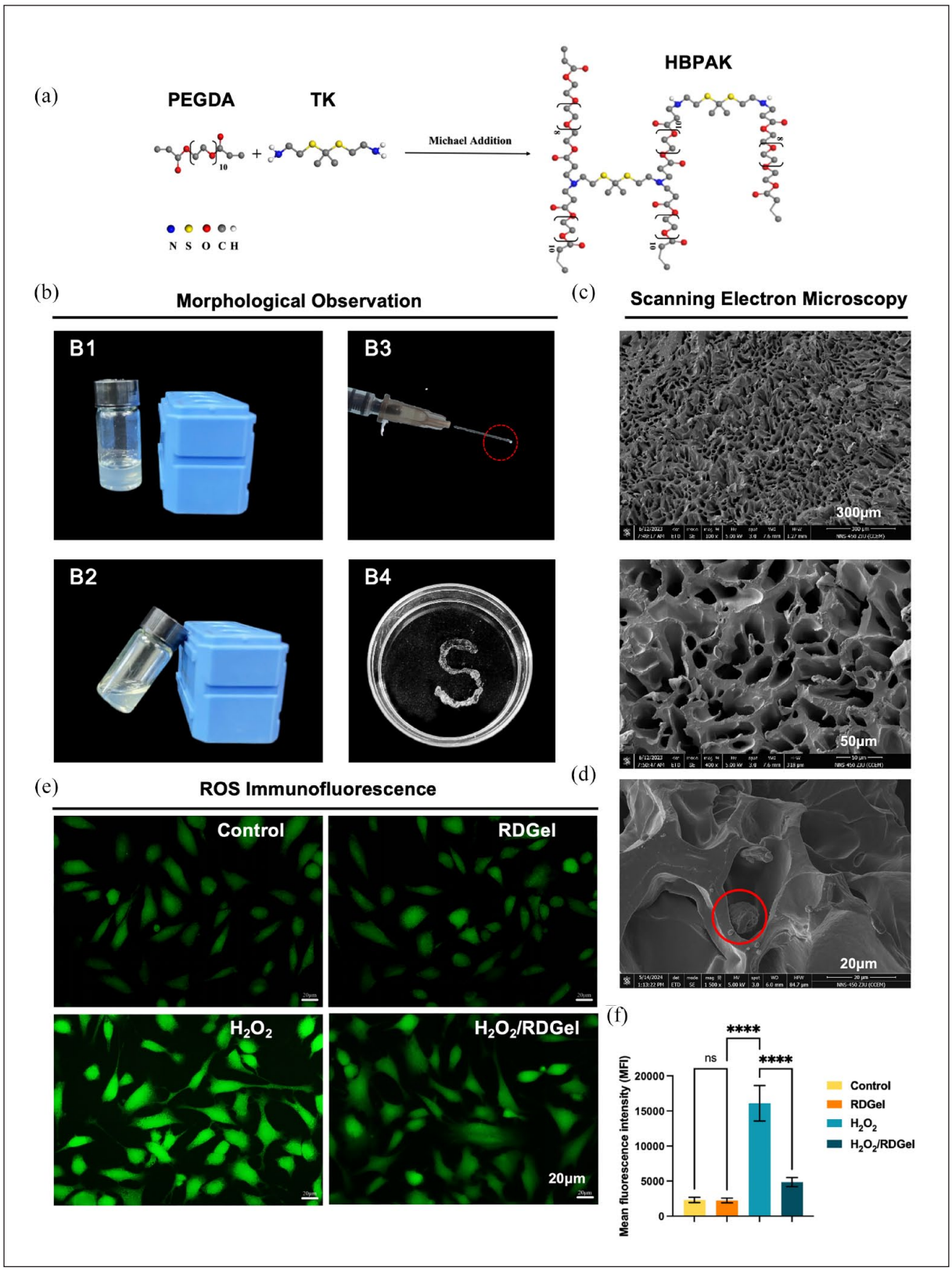

Figure 2. Characterization of 10% RDGel. (a) Schematic plot of HBPAK synthesis. (b) Visualization of the 10% RDGel. (B1–B2). The flowability of 10% RDGel; (B3-B4). The injectability of 10% RDGel. (c) SEM images of the lyophilized 10% RDGel. (d) DPSCs-laden RDGel was incubated for 1 d. Red circle point to cells. (e) Intracellular ROS fluorescence intensity of DPSCs for 1 d. (f) Quantification of cells showing green fluorescence (corresponding to DCFH-DA). Mean ± SD is shown. $n = 3$. p-values are calculated using the one-way ANOVA with Tukey's post-test correction, ****$p < 0.0001$; ns, no significant difference.

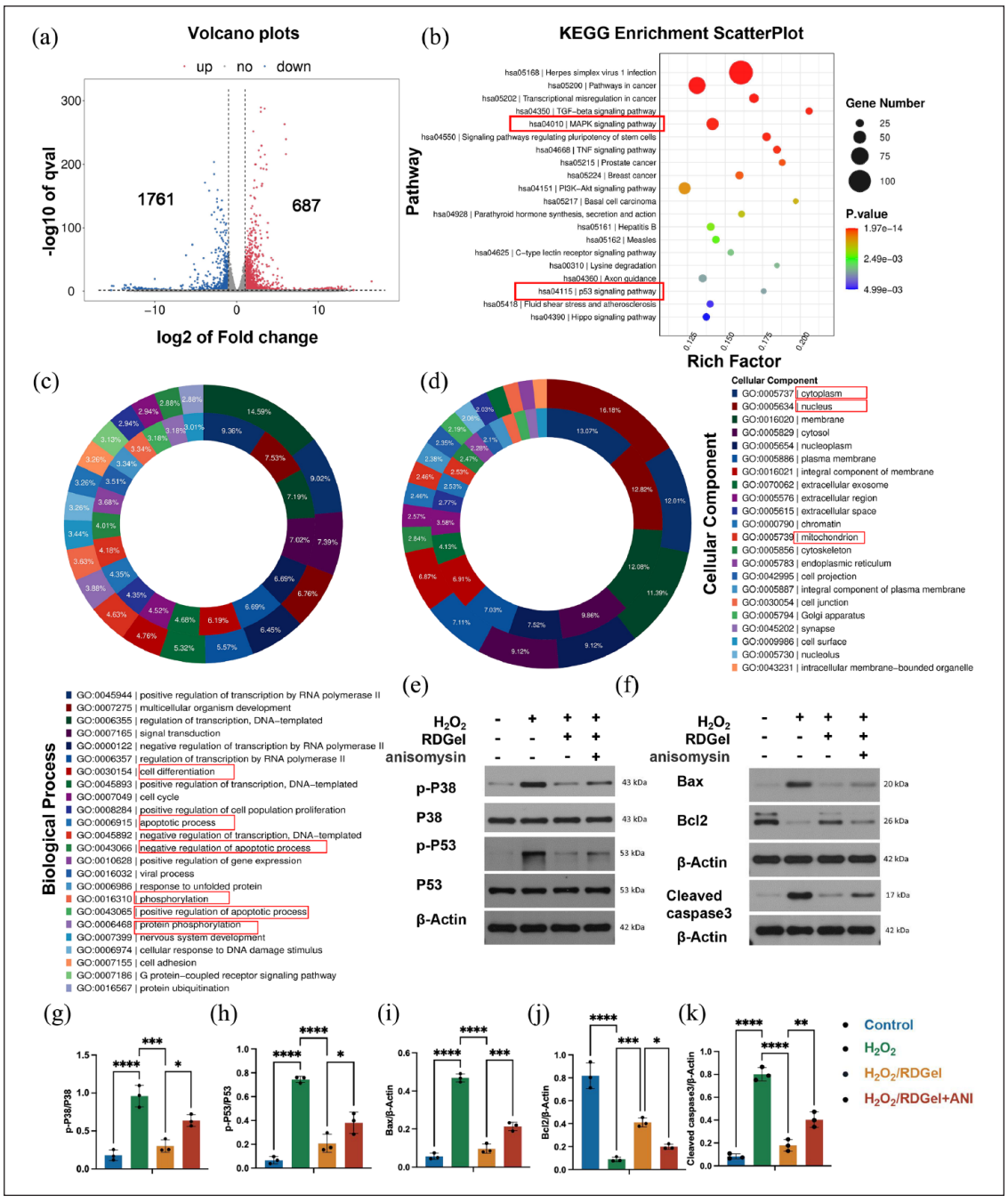

Figure 3. Gene enrichment analysis revealed the significant pathways associated with DPSCs with RDGel encapsulation in oxidative microenvironment. (a)Volcano plots of differentially expressed genes (DEGs) between H_2O_2 and H_2O_2/RDGel group. Blue represents downregulated genes, and red represents upregulated genes. (b) Kyoto Encyclopedia of Genes and Genomes (KEGG) pathway enrichment analysis on differentially expressed genes between the H_2O_2 and H_2O_2/RDGel groups, and the Top 20 pathways are shown. (c) Donut plots are used to show the biological process term with the most up-regulated or down-regulated gene. (d) Donut plots are used to show the cellular component term with the most up-regulated or down-regulated gene. The outer circle is the top 20 biological process or cellular component with the largest number of up-regulated genes, and the inner circle is the top 20 biological process or cellular component with the largest number of down-regulated genes. The screening criteria for differential genes was set as log2FC $\geq$ 1 and $q < 0.05$. (e and f) Representative immunoblotting of pro-apoptotic and anti-apoptotic proteins in DPSCs treated with RDGel or P38 agonist under H_2O_2 stimulation. Control group: DPSCs were cultured in normal for 48 h; H_2O_2 group: DPSCs cultured in ROS microenvironment induced by 200 μM H_2O_2 for 24 h, and then cultured in normal medium for 24 h; H_2O_2/RDGel group: DPSCs cultured in ROS microenvironment induced by 200 μM H_2O_2 with 10% RDGel for 24 h, and then cultured in normal medium with 10% RDGel for 24 h; H_2O_2/RDGel + ANI group: DPSCs cultured in ROS microenvironment induced by 200 μM H_2O_2 with 10% RDGel for 24 h, and then cultured in normal medium with RDGel and the P38 MAPK activator (ANI, 2 μM) for 24 h. (g–k) Quantitative analysis of p-p38/p38, p-p53/p53, Bcl2, Bax and Cleaved caspase3 in DPSCs. Mean ± SD is shown. $n = 3$. p-values are calculated using the one-way ANOVA with Tukey's post-test correction, *$p < 0.05$. **$p < 0.01$. ***$p < 0.001$. ****$p < 0.0001$.

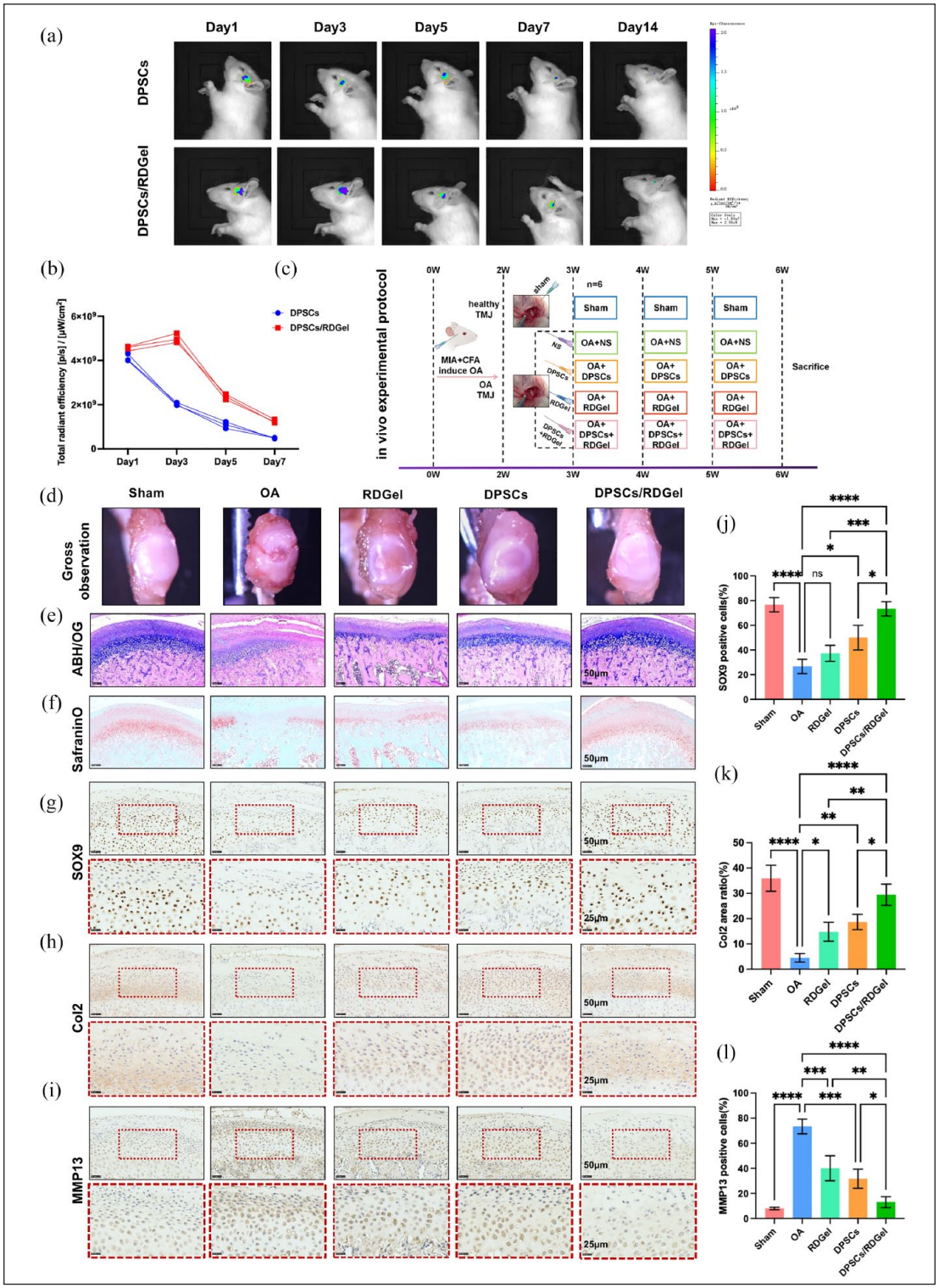

Figure 4. RDGel encapsulation improved the survival of transplanted DPSCs and promoted condylar cartilage repair. (a) Representative bioluminescence images in TMJ at different time points after cell transplantation ($n = 3$ rats per group). (b) Intensity of the bioluminescence signal was quantified as the total radiant efficiency (p/sec/μW/cm^2). (c) Schematic of the injection time points. (d) Macroscopic morphology of the cartilage surfaces after 4-week post-treatment. (e) Representative images of ABH/OG staining of articular cartilages after 4-week post-treatment. (f) Safranin O staining of articular cartilages after 4-week post-treatment. (g) Immunohistochemical staining of SOX9 in articular cartilage. (h) Representative IHC staining for Col2 expression in condylar articular cartilage. (i) Representative IHC staining for MMP13 expression in condylar cartilage. (j–l) Quantification of SOX9, Col2, and MMP13 expression in articular chondrocytes. Data are presented as means ± SD, $n = 6$ rats per group. *P*-values are calculated using the one-way ANOVA with Tukey's post-test correction, *$p < 0.05$. **$p < 0.01$. ***$p < 0.001$. ****$p < 0.0001$; ns, no significant difference.

following the initiation of TMJOA (Figure 4(c)). After 4 weeks, the rats were euthanized for a thorough comprehensive examination of phenotypic changes associated with TMJOA. The OA group exhibited significant condylar articular cartilage erosion, redness, and swelling (Figure 4(d)). Importantly, encapsulation of DPSCs within RDGel showed superior therapeutic efficacy, with more pronounced attenuation of joint swelling and cartilage erosion compared to the DPSCs or RDGel alone. All the three therapeutic groups of DPSCs, RDGel, and DPSCs/RDGel significantly reduced the articular cartilage swelling and joint damage compared to the OA group, demonstrating their anti-inflammatory properties and the synergistic benefits of combining the RDGel with DPSCs in reducing inflammation. Additionally, both the ABH/OG and Safranin O staining revealed a significant loss of proteoglycans in the OA group's articular cartilage, contrasting with the normal expression in the sham group. The OA group also showed pronounced cartilage degeneration with a considerable decrease in proteoglycans and disrupted chondrocyte arrangement. Treatment with either DPSCs or RDGel resulted in a more uniform distribution of proteoglycans in the cartilage layer. Notably, both the ABH/OG and Safranin O staining in the DPSCs/RDGel group showed enhanced cartilage layer integrity, highlighting the synergistic effect of DPSCs/RDGel on condylar cartilage repair (Figure 4(e and f)). In OA, an imbalance in the anabolism and catabolism of chondrocytes disrupts the ECM composition and its viscoelastic properties. To further evaluate the protective effect of DPSCs/RDGel on condylar cartilage ECM, investigation of the expression levels of Sox9, Col2, and MMP13 were analyzed via immunohistochemical staining. The SOX9 gene is expressed during chondrogenesis beginning at the stem cell stage, covering almost all stages of cartilage differentiation. It plays a vital role in activating the expression of Col2. As shown in Figure 4(g) in the DPSCs/RDGel group, the SOX9-positive cells were markedly intensified compared to the OA group. In contrast, the RDGel group did not exhibit a statistically significant improvement in SOX9 expression within the condylar cartilage after 4 weeks of treatment (Figure 4(g and j)). The intricate physical properties of cartilage are governed by the composition of the ECM, a composite network mainly comprised of type II collagen. As expected, the DPSCs/RDGel group notably maintained the expression of Col2 in the TMJOA cartilage layer, while there was no significant difference between the DPSCs and RDGel groups. Notably, Col2 expression was substantially increased in both the DPSCs and RDGel groups compared to the OA group (Figure 4(h and k)). By contrast, the expression of MMP13 was almost undetectable in the normal cartilage, but was dramatically elevated in the OA group. However, in the DPSCs/RDGel group, the number of MMP13-positive cells was dramatically lower than that in the OA group (Figure 4(i and l)). DPSCs/RDGel promotes the expression of anabolic extracellular matrix (ECM) proteins, reduces catabolic ECM protein degradation, and alleviates subchondral bone deterioration in TMJOA.

The subchondral bone plays a crucial role in the pathogenesis of osteoarthritis. To better elucidate the biological effect of RDGel and DPSCs, micro-CT analysis was employed to evaluate the subchondral bone mass and bone microarchitecture in the temporomandibular joint. The parameters such as BV/TV (%) and Tb.N (mm^{-1}) were significantly reduced in the OA group, while the Tb.Sp (mm) was augmented when compared to the sham group, proving the success of TMJOA modeling. RDGel encapsulating DPSCs treatment notably elevated the BV/TV (%) and Tb. N (mm^{-1}) while concurrently attenuating the Tb.Sp (mm). However, the DPSCs or RDGel groups did not exhibit statistical significance compared to the OA group. Such findings collectively supported that the DPSCs/RDGel could ameliorate osteochondral erosion and maintain the structural integrity in TMJOA (Figure S4).

DPSCs/RDGel suppresses inflammatory microenvironment and promotes M2 polarization of macrophages in vivo *and* vitro

To explore the effect of DPSCs/RDGel synergy on TMJOA inflammatory microenvironment *in vivo*, we used immunofluorescence to assess the expression of NADPH Oxidase Type 2 (NOX2), the primary source of ROS and CD86, a marker associated with M1 macrophage polarization. The MIA/CFA induced the upregulated expression of Nox2 protein in condylar synovium and cartilage tissue. In contrast, under normal conditions, only a minute quantity is expressed (Figure 5(a and c)) in the sham group. The DPSCs/RDGel significantly reduced the Nox2 expression in the condylar synovium and cartilage tissue. Similarly, there was almost no expression of CD86 in the sham group in synovium. In addition, the decreased number of $CD86^+$ cells in the DPSCs group and even lower number in the DPSCs/RDGel group demonstrated the anti-inflammatory effect of DPSCs/RDGel *in vivo* (Figure 5(b and d)). Moreover, the DPSCs group exhibited a reduction in the number of $CD86^+$ cells, while an even lower count of $CD86^+$ cells was observed in the DPSCs/RDGel group. A statistical difference was observed between the DPSCs and RDGel groups, indicating a synergistic anti-inflammatory effect of DPSCs/RDGel in *vivo*.

Next, the influence of RDGel, DPSCs, and DPSCs/RDGel on the stimulated macrophages was measured in *vitro*. A material/cell-RAW264.7 co-culture system was established (Figure 5(e)). The immunofluorescence assays was used to detect the expression of M1 (CD86) and M2 (CD206) markers in RAW264.7 cells after co-culture of M1-polarized RAW264.7 cells with DPSCs, RDGel, or DPSCs/RDGel for 1 d. The expression of CD86 decreased,

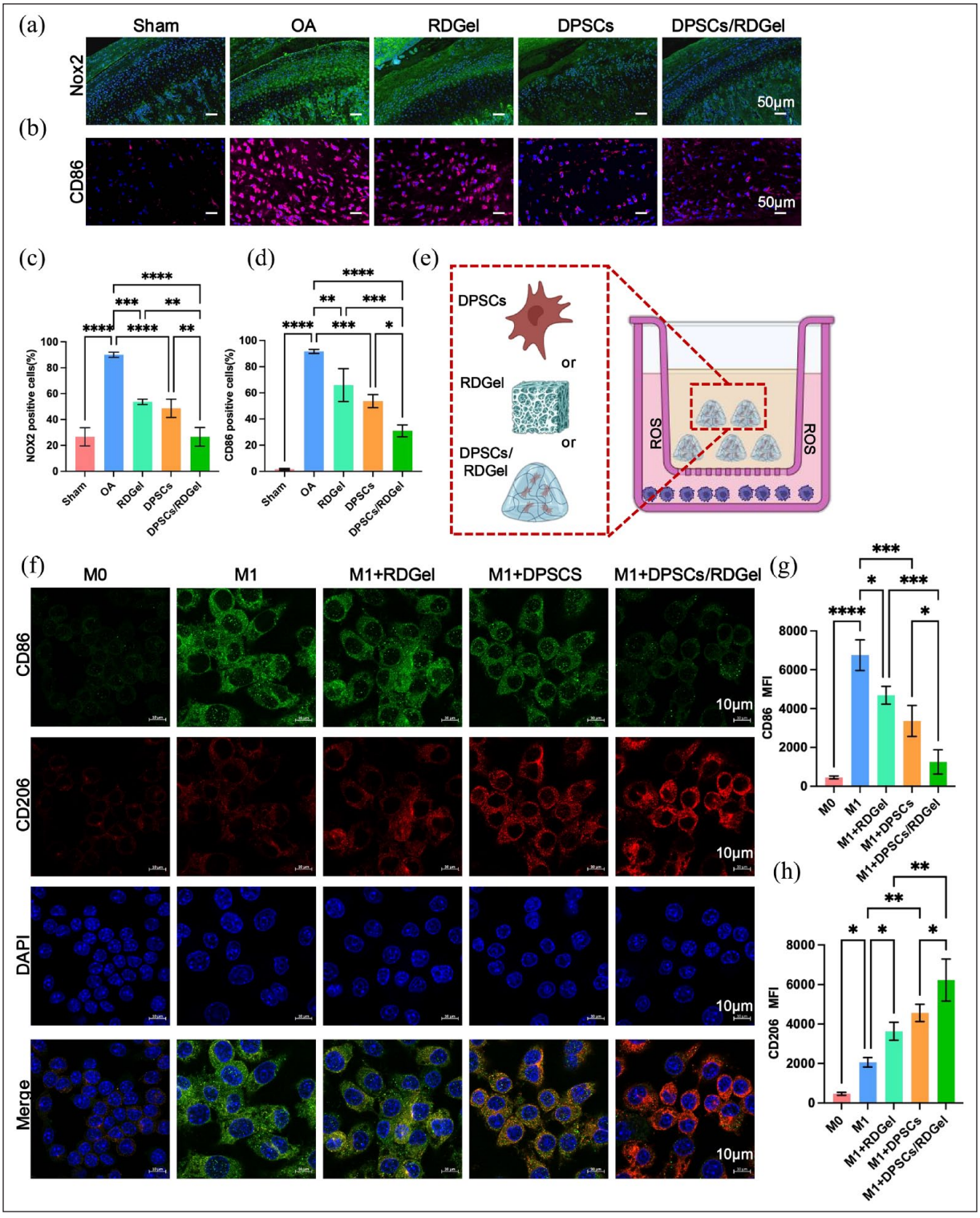

Figure 5. DPSC/RDGel modulated the oxidative stress inflammatory milieu by regulating macrophage polarization, (a) Immunofluorescence staining of NADPH oxidase 2 (marked in green) in condylar cartilage. (b) Representative Immunofluorescence staining for CD86 (marked in red) expression in condylar cartilage. (c and d) Quantification of the expression levels of Nox2 and CD86 in articular cartilage ($n = 6$ rats per group). (e) An in *vitro* stimulation inflammation model diagram showing the cell co-culture under different conditions, where RDGel, DPSCs, or DPSCs/RDGel composite was placed in the upper chamber and different polarization subtypes of RAW264.7 were cultured in the lower chamber. RAW264.7 cells were stimulated by LPS (100 ng/mL) and 10 ng/mL IFN-γ and then treated with RDGel, DPSCs, or DPSCs/RDGel for 1 day. (f) Immunofluorescence staining of CD206 (marked in red) and CD86 (marked in green) in RAW264.7 cells with different polarization subtypes. (g-h) Quantification of the mean fluorescence intensity of CD86 and CD206 in RAW264.7 cells. Mean ± SD is shown. $n = 3$. p-values are calculated using the one-way ANOVA with Tukey's post-test correction, $p < 0.05$. $^{**}p < 0.01$. $^{***}p < 0.001$. $^{****}p < 0.0001$.

while CD206 increased in all the treatment groups. Among them, the M2 polarization of macrophages in the DPSCs/RDGel group was the most pronounced (Figure 5(f–h)), which was consistent with the results in *vivo*. Furthermore, statistical analysis revealed significant differences among all groups.

The flow cytometry results reveal that compared to the M1-polarized Raw264.7 cells treated with the RDGel or DPSCs alone, those co-cultured with the DPSCs/RDGel had significantly lower intracellular ROS intensity (Figure 6(a and b)). The expression of pro-inflammatory cytokines in RAW264.7 cells supernatant from each group, including M0 group, M1 group, RDGel+M1 group, DPSCs+M1 group and DPSCs/RDGel + M1 group, were analyzed by ELISA. This analysis corroborated the upregulation of TNF-α and IL-1β expression in LPS-stimulated macrophages, which was effectively suppressed by the DPSCs/RDGel group. Although the DPSCs or RDGel group demonstrated a certain degree of reduction in pro-inflammatory cytokines, the DPSCs/RDGel group had the lowest levels of TNF-α and IL-1β, indicating notable statistical differences (Figure 6(c and d)). These results indicated that DPSCs/RDGel promoted macrophage polarization from M1 to M2.

Then, the impact of different polarization of macrophages on chondrogenic differentiation of DPSCs was assessed in *vitro*. DPSCs/RAW264.7 co-culture system was established (Figure 6(e)). Furthermore, qPCR analysis revealed that the expression of chondrogenesis-related genes Col2, Sox9, and Aggrecan was significantly suppressed in DPSCs co-cultured with M1 macrophages. In contrast, the expression of these genes was significantly enhanced in the M2 + DPSCs group. Remarkably, the expression of chondroblast-specific genes was significantly upregulated in DPSCs co-cultured with M0 macrophages compared with DPSCs group (Figure 6(f)). Col2, SOX9, and ACAN served as crucial indicators for assessing the chondrogenic differentiation potential of DPSCs. The Western blot results also demonstrated that M2 macrophages effectively promoted the expression of Col2, ACAN, and SOX9, revealing that M2 macrophages had pro-chondrogenic differentiation on DPSCs (Figure 6(g and h)). Western blot results also showed that M2 macrophages could effectively promote the expression of Col2, ACAN, and SOX9, which showed a statistically significant difference compared with M1 group, indicating that M2 macrophages had a role in promoting cartilage differentiation of DPSCs. These findings demonstrate the ability of DPSCs/RDGel to suppress pro-inflammatory cytokine production and promote M2 macrophage polarization, further promoting DPSCs chondrogenic differentiation.

Discussion

Current research highlights the limitations of drug delivery systems for TMJ, particularly the absence of precise localization scaffolds, resulting in undesirable overgrowth in surrounding tissues.[32] However, the efficacy of drug injections in providing long-term relief to patients with TMJOA remains limited. Surgical interventions fail to restore TMJ function fully.[33] In the therapeutic approaches to TMJ repair, the central objective often focuses on cartilage regeneration due to cartilage degeneration under the condition of arthritis or idiopathic condylar resorption, where the significance of tissue engineering is emphasized as an alternative approach.[34,35]

Enhanced post-engraftment cell survival rate has long been a persistent challenge in the application of MSCs. The destabilization of TMJ is intricately associated with oxidative stress.[36,37] However, limited research has explored the utilization of bioactive materials for mitigating ROS in TMJOA therapy. Based on the potential of modulating ROS levels as a therapeutic strategy for TMJOA,[24,38,39] we developed an injectable DPSCs/ROS responsive hydrogel composite system by incorporating HBPAK with the thioketal structure repeating units. HBPAK contains both β-aminoester bonds that are easily hydrolyzed and ketothiol structures that are easily broken in response to ROS. PEGDA serves as a synthetic polymer precursor solution, facilitating the formation of a crosslinked polymeric network upon exposure to light and in the presence of a photoinitiator. The mechanical properties of HBPAK can be modulated by the concentration of PEGDA, which is consistent with other reports.[40] The study conducted by Bai et al.[41] recently highlights the potential of mitochondria-targeting nanozyme injection administered via caudal vein to effectively alleviate TMJOA pain in mice through inhibition of ROS production. While nanozymes are widely acknowledged as promising biomaterials currently under development, our injectable RDGel offers the advantage of minimal invasiveness and suitability for clinical application through intra-articular injection, as opposed to caudal vein injection.[42] This innovative design enabled the hydrogel to respond effectively and eliminate ROS in a hypoxia and inflammatory environment, capitalizing on the ROS sensitivity and resistance to degradation by acids, bases, and proteases of thioketal compounds.[43,44] However, the application of DPSCs binding hydrogels in the TMJOA field is rare. The GelMA hydrogel is a photosensitive biomaterial that exhibits excellent biocompatibility and biodegradability, making it extensively employed in the field of tissue engineering.[45] The study conducted by Shi et al.[46] demonstrated that the incorporation of human salivary histatin-1 into Gel-MA hydrogel exhibited a significant enhancement in promoting TMJ cartilage regeneration. Compared to GelMA, which solely provides a biocompatible three-dimensional environment and facilitates the delivery of bioactive factors, RDGel exhibits the remarkable capability of enhancing the oxidative stress microenvironment. Hydrogel scaffolds exhibit effective interactions with various cells, including BMSCs and chondrocytes, which are commonly employed for TMJ osteochondral repair.[47] Yang

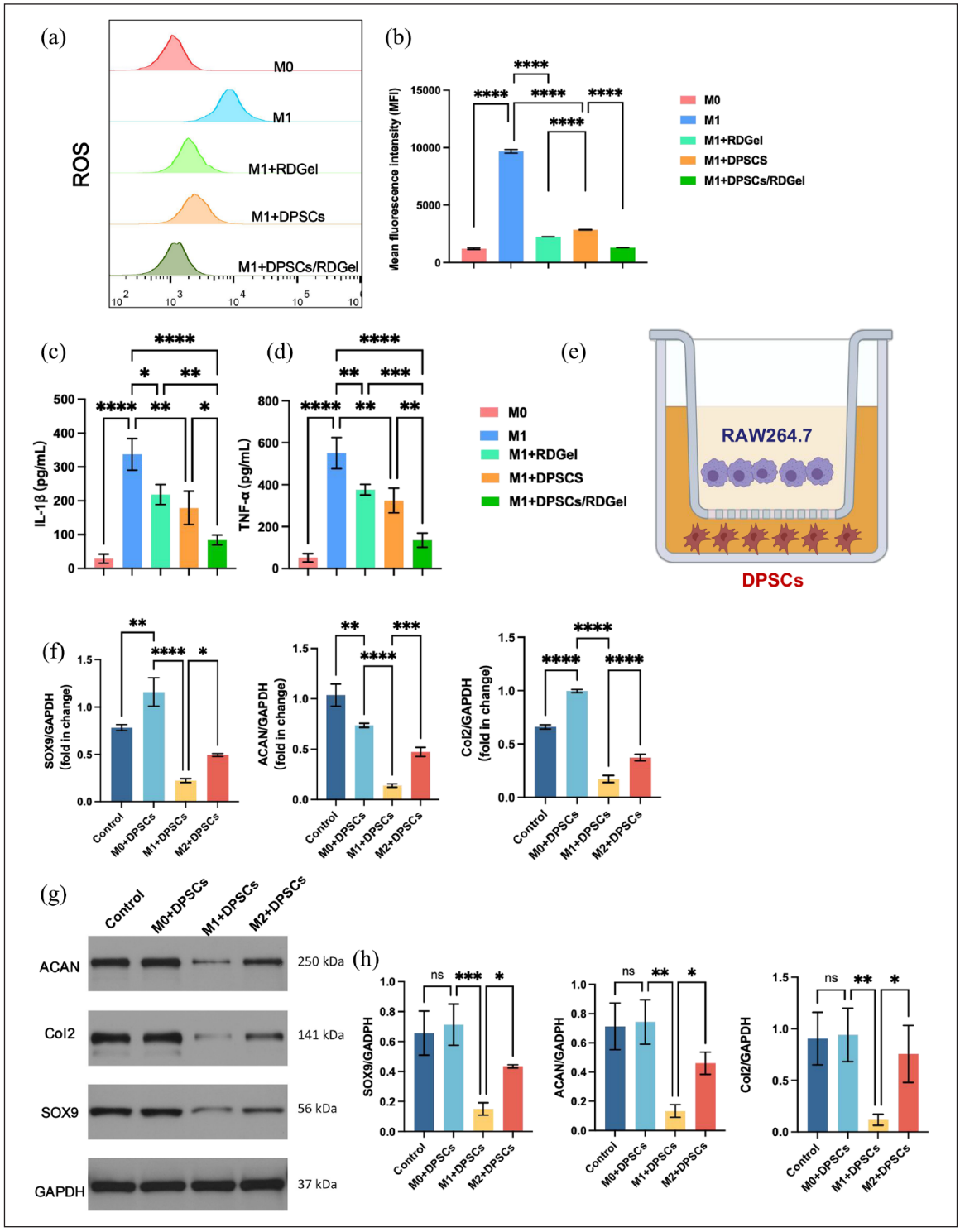

Figure 6. DPSCs/RDGel suppressed inflammation and further enhanced chondrogenic differentiation of DPSCs. (a) Expression level of ROS in RAW264.7 cells at lower transwell chamber from M0, M1, M1 + DPSCs, M1 + RDGel, and M1 + DPSCs/RDGel groups after 1 day co-culture was assessed using flow cytometry. (b) Quantified ROS levels were determined based on the mean fluorescence intensity (MFI). (c and d) TNF-α and IL-1β tested by ELISA assay in the supernatant of RAW264.7 medium from each group collected at 1 day after co-culture. (e) Diagram of RAW264.7 cells of different polarized subgroups co-cultured with DPSCs under different conditions, where the different polarization subtypes of RAW264.7 cell were seeded in the upper chamber, and DPSCs were placed in the lower chamber. The RAW264.7 cells were stimulated with 100 ng/mL of LPS and 10 ng/mL of IFN-γ to differentiate into M1 macrophages. M2 macrophages were derived from RAW267.4 of the M1 + DPSCs/RDGel co-culture group above. (f) mRNA expression of chondroblast differentiation-related genes ACAN, Col2, and SOX9 in DPSCs assessed using RT-PCR. (g and h) Protein expression of ACAN, Col2, and SOX9 in DPSCs. Mean ± SD is shown. $n = 3$. p-values are calculated using the one-way ANOVA with Tukey's post-test correction, $p < 0.05$. $^{**}p < 0.01$. $^{***}p < 0.001$. $^{****}p < 0.0001$; ns, no significant difference.

et al.[4] established that BMSC-coated GelMA microspheres with superwetting properties exhibit enhanced colonization at the bone defect repair site, thereby facilitating the regeneration of TMJOA cartilage. The previous study has demonstrated that double-layer scaffolds loaded with BMSCs/chondrocytes exhibit a significant capacity to enhance fibrocartilage and subchondral bone regeneration, thus offering a promising avenue for mandibular condyle cartilage regeneration.[48] Our study differs from the traditional approach of using BMSCs in cell-loaded hydrogels, which is commonly observed in various TMJOA joint repair studies. The selection of DPSCs for encapsulation is based on their precise embryonic origin and alignment with craniofacial tissue regeneration patterns.[49] This decision is further supported by the understanding that the microenvironment profoundly influences MSC differentiation and bioactivity.[50] Moreover, accumulating evidence suggests that DPSCs exhibit profound immunomodulatory potential compared to BMSCs and demonstrate enhanced anti-apoptotic abilities in the microenvironment characterized by oxidative stress and serum deprivation.[51] In summary, the DPSCs/RDGel composite material represents a synergistic approach, which combines the benefits of ROS-responsive hydrogel component with the regenerative potential of stem cell component. This strategy not only effectively counters inflammation but also offers substantial protection against oxidative damage to the loaded cells, ensuring that the encapsulated DPSCs optimally promote endogenous growth factor production and provide local anti-inflammatory function.

Despite advancements in TMJ cartilage repair using hydrogel scaffolds, there is still limited understanding of how these scaffolds modulate stem cells or chondrocytes.[47] First, in this study, we demonstrated that the RDGel effectively enhanced the anti-apoptotic of DPSCs under H_2O_2-induced oxidative stress in *vitro*. By utilizing the H_2O_2-induced oxidative stress model,[52] transcriptome analysis identified numerous differentially expressed genes associated with apoptosis and cell differentiation. KEGG and GO analyses revealed the potential regulatory mechanism involving MAPK P38/P53 apoptotic signaling cascade. Oxidative stress is known to initiate mitochondrial pathway-mediated apoptosis and elevate ROS levels, triggering stress-induced MAPK pathways and influencing apoptotic and anti-apoptotic signaling cascades.[53] The p38 MAPK, belonging to the family of major MAPKs, is recognized as a class of stress-activated signaling pathways (SAPKs) due to it is always activated by diverse environmental stresses such as oxidative stress, UV irradiation, hypoxia, and so on.[54] The pro-apoptotic effects mediated by p38 cascades have been substantiated as they can upregulate p53 expression by facilitating MDM2 protein degradation, activating the p53-mediated apoptosis pathway.[55,56] Our results showed H_2O_2-induced activated above signaling pathway in DPSCs by the significantly increased expression of p-p38/p38 and p-p53/p53, while DPSCs/RDGel composite could significantly inhibit the expression of the above proteins. The recent study demonstrated that the activation of the MAPK signaling pathway by Zeolite imidazolate framework-8 (ZIF-8) effectively reduced apoptosis of DPSCs. Additionally, incorporating ZIF-8 into a GelMA has been shown to enhance nerve repair in rats with spinal cord injury.[57] The aforementioned findings collectively demonstrate the pivotal role of MAPK P38 in the regulation of apoptosis in DPSCs mediated by bioactive materials. The activation of Cleaved caspase3 serves as a definitive indicator of apoptosis, while the dysregulated equilibrium between the expression levels of anti-apoptotic protein Bcl2 and pro-apoptotic protein Bax can instigate the initiation of the caspase cascade reaction to orchestrate apoptotic processes.[58] Our study confirmed that the activation of Bax by H_2O_2, a pro-apoptotic protein in the Bcl2 family, antagonized the anti-apoptotic protein Bcl2, leading to the alteration of the mitochondrial outer membrane permeabilization. This process resulted in the release of cytochrome C, which then promoted apoptosome formation, triggering Caspase-3-mediated substrate degradation and ultimately inducing apoptosis. More importantly, RDGel encapsulating could significantly decrease the expression of cleaved caspase3 and increase the expression of Bcl2/Bax in DPSCs under oxidative stress. In summary, our findings demonstrate that RDGel encapsulation confers a certain degree of protection against oxidative stress on DPSCs in *vitro.*

Next, in our study, we used the MIA/CFA-induced TMJOA rat model, a well-established and extensively utilized animal model,[59] to study the pathogenesis of OA and evaluate the protective effect of DPSCs/RDGel in *vivo*. We demonstrated that DPSCs encapsulated in RDGel had a notably higher survival rate over the entire time course in *vivo*. Notably, the mean fluorescence intensity of the DPSCs/RDGel group showed an augmentation on day 3, followed by a decline. This phenomenon suggests that the encapsulated DPSCs require time to fully integrate and fuse with the articular cartilage surface to receive the bioluminescent matrix, leading to delayed luminescence. Consistent with previous studies indicating that multiple injections of BMSCs may be more effective than a single injection for treating TMJOA,[60] we administered weekly injections of DPSCs to continuously supply the lesions with DPSCs for sustained efficacy. We observed the most significant recovery in condylar articular cartilage morphology in the DPSCs/RDGel group, suggesting that the synergistic effect of the RDGel encapsulating DPSCs contributed to the attenuation of TMJ OA progression. The DPSCs/RDGel exhibited a synergistic effect in inhibiting cartilage matrix catabolism while enhancing cartilage matrix anabolism. The mandibular condyle is a fibrocartilage structure primarily composed of collagens II.[35] Fibrochondrocytes, involved in the degradation of

the condylar cartilage matrix induced during inflammation, play a crucial role primarily through the synthesis and activation of MMPs.[61] Consequently, suppressing the elevated expression of MMP13 in condylar cartilage is vital to ameliorating cartilage degradation in inflammatory TMJ diseases. A previous study demonstrates that localized DPSC administration can effectively inhibit the expression of MMP3 and MMP13 expression, yielding therapeutic effects on progressive TMJ arthritis.[20] Our study further validated these findings, highlighting that the DPSCs/RDGel group exhibited a significant inhibitory effect on MMP13 expression compared to the OA group while concurrently showing upregulated expression of Col2 and SOX9, which was not observed within either the DPSCs or RDGel group alone. Although stem cells exhibit cartilage repair and immunomodulatory effects, their biological activity may be interfered with by oxidative stress conditions, thus limiting their tissue regeneration effects.[3] Our finding underscores the hypothesis that the delivery of DPSCs via RDGel can enhance the repair of condylar cartilage in *vivo*. However, the exact mechanism of RDGel enhanced cartilage repair in an improved inflammatory environment still requires further exploration.

In further, we observed the DPSCs/RDGel composite significantly improved the inflammatory microenvironment associated with TMJOA in *vivo*. NOX is associated with abnormal ROS production.[62] Previous study revealed the expression of NOX2 was found to be upregulated in IL-1β-treated and OA chondrocytes. In a post-traumatic OA model, pharmacological inhibition of NOX protects rats from developing OA by modulating oxidative stress levels and suppressing MMP-13 expression in chondrocytes.[38] Consistently, our study demonstrated that the DPSCs/RDGel composite could significantly downregulate the overexpression of NOX2 in the MIA/CFA induced TMJ microenvironment in rats, thus ameliorating the oxidative stress inflammatory microenvironment. Importantly, macrophages, which are highly plastic and can switch phenotypes according to the tissue microenvironment, play a critical role in the inflammatory microenvironment of osteoarthritis.[63] A previous study on MIA-induced arthritis in rats showed robust activation of macrophages, peaking at 2 weeks and diminishing by 8 weeks.[64] In our study, a significant reduction in the M1 polarization phenotype of macrophages was observed in the synovial region of the DPSCs/RDGel group compared to the DPSCs or RDGel group alone in *vivo*.

Compared to other types of stem cells, such as BMSCs, there is limited research on the regulation of macrophage polarization by DPSCs. In order to investigate the impact of DPSCs, RDGel, and their combination on macrophages, we established an in *vitro* co-culture model of DPSCs/RDGel-macrophages in *vitro*. A considerable amount of evidence has shown that activation of Nox2 in LPS-induced RAW264.7 macrophages leads to excessive ROS production and subsequent translocation of the nuclear factor (NF-κB) from the cytoplasm to the nucleus. This process results in upregulating pro-inflammatory factors such as TNF-α and IL-1β.[65–67] Moreover, studies have demonstrated significantly elevated levels of inflammatory cytokines, including IL-1β and TNF-α, in joint fluid compared to healthy controls in OA.[64] Our study revealed that compared with the M1 macrophage co-cultured with DPSCs or RDGel, those co-cultured with DPSCs/RDGel had significantly lower intracellular ROS. Then, we observed a significant attenuation in M1 macrophage and an increase in M2 macrophage co-culture with DPSCs/RDGel when compared to either DPSCs-macrophages or RDGel-macrophages co-culture group. Liu et al.[68] have reported increased levels of IL-1β and TNF-α in the synovial fluid of patients with TMJOA. Our study also demonstrated that the mRNA levels of TNF-α and IL-1β in the macrophage supernatant from DPSCs and RDGel groups were significantly reduced, while the above two indexes were particularly significantly down-regulated in the DPSCs/RDGel group, indicating the synergistic anti-inflammatory effects of DPSCs/RDGel. Yan et al.[69] have shown that DPSCs are more effective than other types of stem cell such as PDLSCs, BMMSCs, and ADSCs in triggering M2 macrophage activation in *vivo*, our comparative findings underscored the superiority of synergistic therapy following RDGel encapsulation. The latest evidence also demonstrates that the combination of zirconia scaffolds and DPSCs exerts a superior regulatory effect on M2 polarization of macrophages compared to DPSCs alone. Compared to the above finding limited to in *vitro* studies,[70] we confirmed the effect of DPSCs/RDGel on promoting macrophage polarization in *vivo*, which is closer to preclinical studies. These findings suggest that the combination of biomaterial scaffolds and DPSCs represents a novel research approach for attenuating inflammation and facilitating M2 macrophage polarization.

Furthermore, it is worth mentioning recent findings regarding regulatory mechanisms and crosstalk between macrophages and MSCs.[71] Some scholars have emphasized the capacity of M1 macrophage to suppress the chondrogenic differentiation of MSCs, while M2 macrophage can stimulate MSCs to differentiate into chondrocytes.[72] Our study provided additional supportive evidence that M1 macrophages inhibits the chondrogenic differentiation of DPSCs and demonstrated that DPSCs/RDGel encapsulation could partially reverse this suppression, preliminarily revealing the interaction between macrophages and DPSCs in the process of cartilage repair. In conclusion, our findings illustrate that the optimized inflammatory microenvironment mediated by DPSCs/RDGel conferred enhanced viability and chondrogenic differentiation of DPSCs in *vivo* and in *vitro*.

Although this study evaluated the efficacy of DPSCs/RDGel in treating TMJ arthritis, further investigation into

the impact of RDGel encapsulation on DPSCs secretion factors may serve as a crucial determinant for elucidating the effect of DPSCs/RDGel on cartilage repair. Despite DPSCs/RDGels have demonstrated enhanced immunomodulatory effects compared to DPSCs, further investigations are needed to comprehensively elucidate the underlying mechanisms.

Conclusion

The DPSCs/RDGel composite was intricately prepared by encapsulating DPSCs within a ROS-responsive injectable multifunctional hydrogel. In our investigation, the treatment group receiving the DPSCs/RDGel composite displayed significantly heightened efficacy in addressing cartilage defects in TMJ rats, surpassing the outcomes observed in groups treated with either DPSCs or RDGel alone. This efficacy is attributed to the dual roles of the composite: RDGel encapsulation augmented the anti-apoptotic capacity of DPSCs under oxidative stress; and notably ameliorated the inflammatory microenvironment of TMJOA. As a result, it increases the engraftment rate of DPSCs in rats TMJ, promotes M2 polarization of macrophages, and further enhances the condylar cartilage repair potential of DPSCs.

Acknowledgements

Special thanks to Cheng Chen from the Public Platform of the Medical Research Center of the Academy of Chinese Medicine of Zhejiang Chinese Medicine University, and Yuansong Yu, Juan Li and Shubo Hu from the Odontogenic Stem Cell Bank and Research and Development Center for their valuable technical support. The authors also express gratitude to Dong Wang for his insightful suggestions and active participation. We express our gratitude to Figdraw and biorender for providing the drawing material.

Author contributions

JM, JL, CG, and HJ conceived the study. JM, YQ, SX, and LX conducted the in vivo experiments. JM and SW tested material samples and performed the in *vitro* assay. YL, JW, and SY conducted the in *vitro* experiments. JM, SY, and LX analyzed the data. JM wrote the original draft, and JL, CG, YL, JW, and HJ revised the manuscript for important intellectual content. CG, JL, and HJ supervised the study. All authors read and approved the final version of the manuscript.

Declaration of conflicting interests

The author(s) declared no potential conflicts of interest with respect to the research, authorship, and/or publication of this article.

Funding

The author(s) disclosed receipt of the following financial support for the research, authorship, and/or publication of this article: The authors acknowledge the support received from the Natural Science Foundation of China (81970978 and 81973869), the Natural Science Foundation of Zhejiang Province (LD22C060002 and LY22H140006).

ORCID iD

Jun Lin https://orcid.org/0000-0002-2431-0121

Supplemental material

Supplemental material for this article is available online.

References

1. Peng BY, Singh AK, Tsai CY, et al. Platelet-derived biomaterial with hyaluronic acid alleviates temporal-mandibular joint osteoarthritis: clinical trial from dish to human. *J Biomed Sci* 2023; 30: 77.
2. Derwich M, Mitus-Kenig M and Pawlowska E. Mechanisms of action and efficacy of hyaluronic acid, corticosteroids and platelet-rich plasma in the treatment of temporomandibular joint osteoarthritis-a systematic review. *Int J Mol Sci* 2021; 22: 7405.
3. Zhao Y and Xie L. An update on mesenchymal stem cell-centered therapies in temporomandibular joint osteoarthritis. *Stem Cells Int* 2021; 2021: 6619527.
4. Yang Y, Huang C, Zheng H, et al. Superwettable and injectable GelMA-MSC microspheres promote cartilage repair in temporomandibular joints. *Front Bioeng Biotechnol* 2022; 10: 1026911.
5. Buzoglu HD, Burus A, Bayazit Y, et al. Stem cell and oxidative stress-inflammation cycle. *Curr Stem Cell Res Ther* 2023; 18: 641–652.
6. Wechsler ME, Rao VV, Borelli AN, et al. Engineering the MSC secretome: a hydrogel focused approach. *Adv Healthc Mater* 2021; 10: e2001948.
7. Yu H, Huang Y and Yang L. Research progress in the use of mesenchymal stem cells and their derived exosomes in the treatment of osteoarthritis. *Ageing Res Rev* 2022; 80: 101684.
8. Matheus HR, Ozdemir SD and Guastaldi FPS. Stem cell-based therapies for temporomandibular joint osteoarthritis and regeneration of cartilage/osteochondral defects: a systematic review of preclinical experiments. *Osteoarthritis Cartilage* 2022; 30: 1174–1185.
9. Linkova N, Khavinson V, Diatlova A, et al. Peptide regulation of chondrogenic stem cell differentiation. *Int J Mol Sci* 2023; 24: 8415.
10. Van Bellinghen X, Idoux-Gillet Y, Pugliano M, et al. Temporomandibular joint regenerative medicine. *Int J Mol Sci* 2018; 19: 446.
11. Divband B, Aghazadeh M, Al-Qaim ZH, et al. Bioactive chitosan biguanidine-based injectable hydrogels as a novel BMP-2 and VEGF carrier for osteogenesis of dental pulp stem cells. *Carbohydr Polym* 2021; 273: 118589.
12. Fageeh HN. Preliminary evaluation of proliferation, wound healing properties, osteogenic and chondrogenic potential of dental pulp stem cells obtained from healthy and periodontitis affected teeth. *Cells* 2021; 10: 2118.
13. Sun Q, Zhuang Z, Bai R, et al. Lysine 68 methylation-dependent SOX9 stability control modulates chondrogenic differentiation in dental pulp stem cells. *Adv Sci* 2023; 10: e2206757.

14. Lee YC, Chan YH, Hsieh SC, et al. Comparing the osteogenic potentials and bone regeneration capacities of bone marrow and dental pulp mesenchymal stem cells in a rabbit calvarial bone defect model. *Int J Mol Sci* 2019; 20: 5015.
15. Bielajew BJ, Donahue RP, Espinosa MG, et al. Knee orthopedics as a template for the temporomandibular joint. *Cell Rep Med* 2021; 2: 100241.
16. Lo Monaco M, Gervois P, Beaumont J, et al. Therapeutic potential of dental pulp stem cells and leukocyte- and platelet-rich fibrin for osteoarthritis. *Cells* 2020; 9: 980.
17. Longoni A, Utomo L, van Hooijdonk IE, et al. The chondrogenic differentiation potential of dental pulp stem cells. *Eur Cell Mater* 2020; 39: 121–135.
18. Pouraghaei Sevari S, Ansari S, Chen C and Moshaverinia A. Harnessing dental stem cell immunoregulation using cell-laden biomaterials. *J Dent Res* 2021; 100: 568–575.
19. Cavalcanti BN, Zeitlin BD and Nor JE. A hydrogel scaffold that maintains viability and supports differentiation of dental pulp stem cells. *Dent Mater* 2013; 29: 97–102.
20. Cui SJ, Zhang T, Fu Y, et al. DPSCs attenuate experimental progressive TMJ arthritis by inhibiting the STAT1 pathway. *J Dent Res* 2020; 99: 446–455.
21. Smojver I, Katalinic I, Bjelica R, et al. Mesenchymal stem cells based treatment in dental medicine: a narrative review. *Int J Mol Sci* 2022; 23: 1662.
22. Weng Z, Wang Y, Ouchi T, et al. Mesenchymal stem/stromal cell senescence: hallmarks, mechanisms, and combating strategies. *Stem Cells Transl Med* 2022; 11: 356–371.
23. Choi DH, Lee KE, Oh SY, et al. Tonsil-derived mesenchymal stem cells incorporated in reactive oxygen species-releasing hydrogel promote bone formation by increasing the translocation of cell surface GRP78. *Biomaterials* 2021; 278: 121156.
24. Zhang Z, Yuan L, Liu Y, et al. Integrated cascade nanozyme remodels chondrocyte inflammatory microenvironment in temporomandibular joint osteoarthritis via inhibiting ROS-NF-kappaB and MAPK pathways. *Adv Healthc Mater* 2023; 12: e2203195.
25. Arra M, Swarnkar G, Ke K, et al. LDHA-mediated ROS generation in chondrocytes is a potential therapeutic target for osteoarthritis. *Nat Commun* 2020; 11: 3427.
26. Bolduc JA, Collins JA and Loeser RF. Reactive oxygen species, aging and articular cartilage homeostasis. *Free Radic Biol Med* 2019; 132: 73–82.
27. Jun SK, Yoon JY, Mahapatra C, et al. Ceria-incorporated MTA for accelerating odontoblastic differentiation via ROS downregulation. *Dent Mater* 2019; 35: 1291–1299.
28. Ha CW, Park YB, Kim SH and Lee HJ. Intra-articular mesenchymal stem cells in osteoarthritis of the knee: a systematic review of clinical outcomes and evidence of cartilage repair. *Arthroscopy* 2019; 35: 277–288 e272.
29. Hasani-Sadrabadi MM, Sarrion P, Pouraghaei S, et al. An engineered cell-laden adhesive hydrogel promotes craniofacial bone tissue regeneration in rats. *Sci Transl Med* 2020; 12: eaay6853.
30. Ji X, Yuan X, Ma L, et al. Mesenchymal stem cell-loaded thermosensitive hydroxypropyl chitin hydrogel combined with a three-dimensional-printed poly(epsilon-caprolactone) /nano-hydroxyapatite scaffold to repair bone defects via osteogenesis, angiogenesis and immunomodulation. *Theranostics* 2020; 10: 725–740.
31. Tian B, Liu J, Guo S, et al. Macromolecule-based hydrogels nanoarchitectonics with mesenchymal stem cells for regenerative medicine: a review. *Int J Biol Macromol* 2023; 243: 125161.
32. Qiu J, Hua B, Ye X and Liu X. Intra-articular injection of kartogenin promotes fibrocartilage stem cell chondrogenesis and attenuates temporomandibular joint osteoarthritis progression. *Front Pharmacol* 2023; 14: 1159139.
33. Chen D, Wu JY, Kennedy KM, et al. Tissue engineered autologous cartilage-bone grafts for temporomandibular joint regeneration. *Sci Transl Med* 2020; 12:eabb6683.
34. Zhang W, Zeng L, Yu H, et al. Injectable spontaneous hydrogen-releasing hydrogel for long-lasting alleviation of osteoarthritis. *Acta Biomater* 2023; 158: 163–177.
35. Cardoneanu A, Macovei LA, Burlui AM, et al. Temporomandibular joint osteoarthritis: pathogenic mechanisms involving the cartilage and subchondral bone, and potential therapeutic strategies for joint regeneration. *Int J Mol Sci* 2022; 24: 171.
36. Han S. Osteoarthritis year in review 2022: biology. *Osteoarthritis Cartilage* 2022; 30: 1575–1582.
37. Ye T, He F, Lu L, et al. The effect of oestrogen on mandibular condylar cartilage via hypoxia-inducible factor-2alpha during osteoarthritis development. *Bone* 2020; 130: 115123.
38. Han J, Park D, Park JY and Han S. Inhibition of nadph oxidases prevents the development of osteoarthritis. *Antioxidants* 2022; 11: 2346.
39. Zhen J, Chen X, Mao Y, et al. GLX351322, a novel NADPH oxidase 4 inhibitor, attenuates TMJ osteoarthritis by inhibiting the ROS/MAPK/NF-kappaB signaling pathways. *Oxid Med Cell Longev* 2023; 2023: 1952348.
40. Trucco D, Vannozzi L, Teblum E, et al. Graphene oxide-doped gellan gum-PEGDA bilayered hydrogel mimicking the mechanical and lubrication properties of articular cartilage. *Adv Healthc Mater* 2021; 10: e2001434.
41. Bai Q, Zhou Y, Cui X, et al. Mitochondria-targeting nanozyme alleviating temporomandibular joint pain by inhibiting the TNFalpha/NF-kappaB/NEAT1 pathway. *J Mater Chem B* 2023; 12: 112–121.
42. Atwal A, Dale TP, Snow M, et al. Injectable hydrogels: an emerging therapeutic strategy for cartilage regeneration. *Adv Colloid Interface Sci* 2023; 321: 103030.
43. Wu S, Zhang H, Wang S, et al. Ultrasound-triggered in situ gelation with ROS-controlled drug release for cartilage repair. *Mater Horiz* 2023; 10: 3507–3522.
44. Zhai Z, Ouyang W, Yao Y, et al. Dexamethasone-loaded ROS-responsive poly(thioketal) nanoparticles suppress inflammation and oxidative stress of acute lung injury. *Bioact Mater* 2022; 14: 430–442.
45. Sun H, Xu J, Wang Y, et al. Bone microenvironment regulative hydrogels with ROS scavenging and prolonged oxygen-generating for enhancing bone repair. *Bioact Mater* 2023; 24: 477–496.
46. Shi C, Yao Y, Wang L, et al. Human salivary histatin-1-functionalized gelatin methacrylate hydrogels promote the regeneration of cartilage and subchondral bone in temporomandibular joints. *Pharmaceuticals* 2021; 14: 484.
47. Wang X, Liu F, Wang T, et al. Applications of hydrogels in tissue-engineered repairing of temporomandibular joint diseases. *Biomater Sci* 2024; 12: 2579–2598.

48. Wang H, Xu Y, Wang P, et al. Cell-mediated injectable blend hydrogel-BCP ceramic scaffold for in situ condylar osteochondral repair. *Acta Biomater* 2021; 123: 364–378.
49. Tatullo M, Marrelli M, Shakesheff KM, et al. Dental pulp stem cells: function, isolation and applications in regenerative medicine. *J Tissue Eng Regen Med* 2015; 9: 1205–1216.
50. Lagneau N, Tournier P, Nativel F, et al. Harnessing cell-material interactions to control stem cell secretion for osteoarthritis treatment. *Biomaterials* 2023; 296: 122091.
51. Zhang Y, Xing Y, Jia L, et al. An in vitro comparative study of multisource derived human mesenchymal stem cells for bone tissue engineering. *Stem Cells Dev* 2018; 27: 1634–1645.
52. Alaidaroos NYA, Alraies A, Waddington RJ, et al. Differential SOD2 and GSTZ1 profiles contribute to contrasting dental pulp stem cell susceptibilities to oxidative damage and premature senescence. *Stem Cell Res Ther* 2021; 12: 142.
53. Snieckute G, Ryder L, Vind AC, et al. ROS-induced ribosome impairment underlies ZAKalpha-mediated metabolic decline in obesity and aging. *Science* 2023; 382: eadf3208.
54. Sanz-Ezquerro JJ and Cuenda A. p38 signalling pathway. *Int J Mol Sci* 2021; 22: 1003.
55. Whitaker RH and Cook JG. Stress relief techniques: p38 MAPK determines the balance of cell cycle and apoptosis pathways. *Biomolecules* 2021; 11: 1444.
56. Yue J and Lopez JM. Understanding MAPK signaling pathways in apoptosis. *Int J Mol Sci* 2020; 21: 2346.
57. Zhou H, Jing S, Xiong W, et al. Metal-organic framework materials promote neural differentiation of dental pulp stem cells in spinal cord injury. *J Nanobiotechnology* 2023; 21: 316.
58. Korotkov SM. Mitochondrial oxidative stress is the general reason for apoptosis induced by different-valence heavy metals in cells and mitochondria. *Int J Mol Sci* 2023; 24: 14459.
59. Wang D, Qi Y, Wang Z, et al. Recent advances in animal models, diagnosis, and treatment of temporomandibular joint osteoarthritis. *Tissue Eng Part B Rev* 2023; 29: 62–77.
60. Lu L, Zhang X, Zhang M, et al. RANTES and SDF-1 are keys in cell-based therapy of TMJ osteoarthritis. *J Dent Res* 2015; 94: 1601–1609.
61. Lu K, Ma F, Yi D, et al. Molecular signaling in temporomandibular joint osteoarthritis. *J Orthop Transl* 2022; 32: 21–27.
62. Vermot A, Petit-Härtlein I, Smith SME, et al. NADPH oxidases (NOX): an overview from discovery, molecular mechanisms to physiology and pathology. *Antioxidants* 2021; 10: 890.
63. Zhang Y and Ji Q. Macrophage polarization in osteoarthritis progression: a promising therapeutic target. *Front Cell Dev Biol* 2023; 11: 1269724.
64. Xie J, Huang Z, Yu X, et al. Clinical implications of macrophage dysfunction in the development of osteoarthritis of the knee. *Cytokine Growth Factor Rev* 2019; 46: 36–44.
65. Cheng CS, Zou Y and Peng J. Oregano essential oil attenuates RAW264.7 cells from lipopolysaccharide-induced inflammatory response through regulating NADPH oxidase activation-driven oxidative stress. *Molecules* 2018; 23: 1857.
66. Wang B, Wang Y, Zhang J, et al. ROS-induced lipid peroxidation modulates cell death outcome: mechanisms behind apoptosis, autophagy, and ferroptosis. *Arch Toxicol* 2023; 97: 1439–1451.
67. Zhao YX, Wang LY, Liu MW, et al. ROS inhibition increases KDM6A-mediated NOX2 transcription and promotes macrophages oxidative stress and M1 polarization. *Cell Stress Chaperon* 2023; 28: 375–384.
68. Liu C, Zhang L, Zheng X, et al. Pleiotrophin inhibited chondrogenic differentiation potential of dental pulp stem cells. *Oral Dis* 2023; 30: 1439–1450.
69. Yang Z, Ma LS, Du CL, et al. Dental pulp stem cells accelerate wound healing through CCL2-induced M2 macrophages polarization. *Iscience* 2023; 26: 108043.
70. Liu BY, He MD, Chen B, et al. Identification of key pathways in zirconia/dental pulp stem cell composite scaffold-mediated macrophage polarization through transcriptome sequencing. *Biotechnol Genet*. Epub ahead of print 21 March 2023. DOI: 10.1080/02648725.2023.2191080.
71. Fahy N, de Vries-van Melle ML, Lehmann J, et al. Human osteoarthritic synovium impacts chondrogenic differentiation of mesenchymal stem cells via macrophage polarisation state. *Osteoarthr Cartilage* 2014; 22: 1167–1175.
72. Wang L, Li S, Xiao H, et al. TGF-beta1 derived from macrophages contributes to load-induced tendon-bone healing in the murine rotator cuff repair model by promoting chondrogenesis. *Bone Joint Res* 2023; 12: 219–230.